Mechanism of Allosteric Regulation of Dnmt1's Processivity†

Željko M. Svedružić# and Norbert O. Reich*

Department of Chemistry and Biochemistry and Program in Biomolecular Science and Engineering, University of California, Santa Barbara, California 93106

Received May 26, 2005; Revised Manuscript Received August 11, 2005

ABSTRACT: We have analyzed the relationship between the allosteric regulation and processive catalysis of DNA methyltransferase 1 (Dnmt1). Processivity is described quantitatively in terms of turnover rate, DNA dissociation rate, and processivity probability. Our results provide further evidence that the active site and the allosteric sites on Dnmt1 can bind DNA independently. Dnmt1's processive catalysis on unmethylated DNA is partially inhibited when the allosteric site binds unmethylated DNA and fully inhibited when the allosteric site binds a single-stranded oligonucleotide inhibitor. The partial inhibition by unmethylated DNA is caused by a decrease in the turnover rate and an increase in the substrate DNA dissociation rate. Processive catalysis with premethylated DNA is not affected if the allosteric site is exposed to premethylated DNA but is fully inhibited if the allosteric site binds unmethylated DNA or poly(dA-dT). In sum, the occupancy of the allosteric site modulates the enzyme's commitment to catalysis, which reflects the nature of the substrate and the DNA bound at the allosteric site. Our in vitro results are consistent with the possibility that the processive action of Dnmt1 may be regulated in vivo by specific regulatory nucleic acids such as DNA, RNA, or poly(ADP-ribose).

Mammalian DNA methylation is an essential component of epigenetic chromatin reorganization processes that regulate gene silencing, oncogene activation, tumor suppressor inactivation, DNA repair, viral infection, early development, cell differentiation, and DNA recombination (*1*−*3*). Several mammalian DNA methyltransferases have been identified (*4*−*6*) yet remain poorly characterized due to their complex kinetic properties and exceptionally slow catalytic turnover rates (*6*−*8*). The large, 1620-residue DNA methyltransferase 1 (Dnmt1)[1] enzyme is the best characterized (*7*, *9*−*14*) and is composed of a small C-terminal catalytic domain (residues 1102−1620) and a large regulatory domain (residues 1−1101) (*10*, *15*, *16*). The catalytic domain shows structural similarities with the small bacterial DNA cytosine methyltransferases, while the regulatory domain is in many aspects unique and less understood.

The sequence homology with pyrimidine methyltransferases indicates that the small catalytic domain includes the AdoMet binding domain and the active site (*17*). Inhibition by the mechanism-based inactivator 5-fluoro-cytosine (*18*) and the ability to catalyze the exchange of the cytosine C^5 hydrogen (*19*) suggest that Dnmt1 and other pyrimidine methyltransferases share a common catalytic mechanism (Figure 1 and ref *20*). Dnmt1 activates the target base prior to the methyltransfer step by reversible formation of a covalent intermediate with the target base (Figure 1 and ref

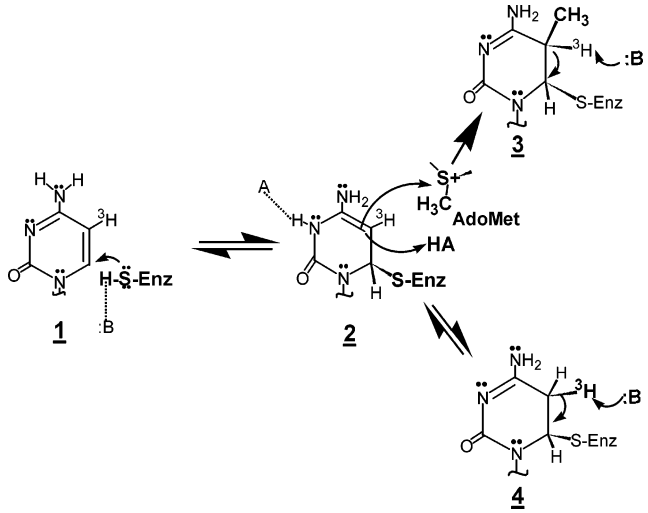

FIGURE 1: Enzyme activity assays for Dnmt1 (*19*). Methylation (as in Figure 8) is followed using radiolabeled AdoMet. A slight variation is the ^3H release assay (as in Figures 3−7), where unlabeled AdoMet is used with DNA tritiated at the cytosine C^5 position, and tritium release is followed (**2** → **3**). This allows the enzymes activity to be followed with labeled and unlabeled DNA mixtures (depicted in Figure 2 and given in Figures 4−7). The ^3H exchange assay (**2** → **4**) is similar to the release assay but done without AdoMet or in the presence of AdoMet analogues; this separates product formation (5-methylcytosine) steps from the enzyme's attack onto the target base (**1** → **2**, see data in Figure 9).

† This work was supported by NIH GM56289 to N.O.R.

* To whom correspondence should be addressed. Tel: 805-893-8368. FAX 805-893-4120. E-mail reich@chem.ucsb.edu.

Current address: School of Molecular Biosciences, Department of Biophysics and Biochemistry, Washington State University, Pullman, WA 99164.

[1] Abbreviations: AdoMet, *S*-adenosyl-L-methionine; bp, base pair; C^5,C^2,C^4 etc., carbon five, carbon two, etc. of the target base; ^{5m}C, 5-methyl-2′deoxycytosine; dCTP, deoxycytosine triphosphate; poly(dG-dC), double-stranded alternating polymer of deoxyguanine and deoxycytosine; dITP, deoxyinosine triphosphate; Dnmt1, DNA methyltransferase 1; k_{off}, rate constant for the enzyme−DNA dissociation; poly(dI-dC), double-stranded alternating polymer of deoxyinosine and deoxycytosine; pm-poly(dG-dC) or pm-poly(dI-dC), premethylated poly(dG-dC) or poly(dI-dC); sin, sinefungin.

10.1021/bi050988f CCC: $30.25
Published on Web 10/22/2005

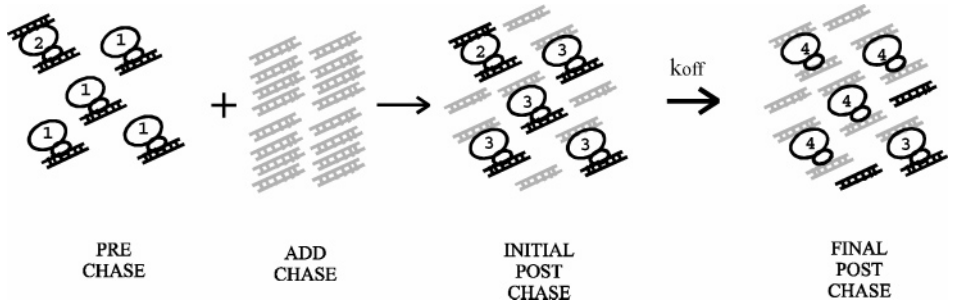

FIGURE 2: Schematic showing the chase experiments following tritium release. At the start of the chase experiments (PRE CHASE), the hot reaction is prepared by adding Dnmt1 (oval shapes) and ^{3}H-labeled DNA (black rail) in a concentration ratio that gives only a mild substrate inhibition (*19*). This ensures the presence of a mixture of Dnmt1 with only the active site occupied (**1**) and with both the active and allosteric sites occupied (**2**). The reaction is initiated by adding AdoMet, and the measured ^{3}H release rates derive from the combined activity of forms **1** and **2**. The chase reaction is started after the first few turnovers by adding a large excess (*n*-fold) of unlabeled DNA (gray rail) to an aliquot of the labeled reaction mixture. Unlabeled DNA can have the same or different sequence than the substrate DNA. Adding an excess of unlabeled DNA results in the immediate occupancy of unoccupied DNA binding sites (transition between forms **1**→**3**, INITIAL POST CHASE). If Dnmt1 is processive, the turnover rates (k, eq 6) will be much faster than the dissociation rate constant for the labeled DNA (k_{off}, eq 6). Thus, the labeled DNA will stay bound at the active site through the subsequent turnovers and the ^{3}H release rates will reflect the combined catalytic activity from forms **2** and **3**. If Dnmt1 is not processive, the dissociation rate for the labeled DNA at the active site (k_{off}, eq 6) is faster than the turnover rates (k, eq 6), and the labeled DNA will dissociate from the active site before the next turnover. Thus, the measured ^{3}H release rates will be only nth fraction of the original rates since most of the Dnmt1 molecules will be in ^{3}H exchange silent form (**4**, FINAL POST CHASE). Further details about the assay design are presented at the start of the results section.

20). Dnmt1 and the bacterial enzyme M·HhaI share catalytic intermediates, the rate-limiting step, and some key features that ensure stability of the activated target base (*19*).

The N-terminal regulatory domain is unique for Dnmt1. It contains part of a sequence that binds the methylation target site (*21*), an allosteric site that binds nucleic acids (*10*, *22*), and sequence motifs that support interaction with other proteins (*4*, *23*). There is also a phosphorylation site at Ser 514 (*24*) within the sequence that targets Dnmt1 to the DNA replication foci (*25*). Dnmt1 mutants lacking portions of the N-terminal regulatory domain show faster rates than the wild-type Dnmt1 with all DNA substrates (*10*). Thus, the N-terminal regulatory domain inhibits Dnmt1 activity, and the mechanism and extent of inhibition depend on DNA sequence, methylation state, and structure (*10*, *13*, *26*). Unmethylated DNA substrates show partial inhibition at higher substrate concentrations consistent with a gradual occupancy of the active site and allosteric site (*13*, *19*). In contrast, no distinct inhibition is observed with premethylated substrates, which have at least one ^{5m}C positioned within the enzyme's footprint from the target cytosine (*14*, *19*, *26*). A GC-rich 30-nucleotide single-stranded sequence (*13*) fully inhibits Dnmt1 in vitro (K_i close to 30 nM) and DNA methylation in cells (*13*). Interestingly, the inhibitor's potency is 2 orders of magnitude lower if its single ^{5m}C site is replaced with cytosine (*13*). This methylation-dependent inhibition may be unique for *single-stranded* DNA because no such methylation-dependent enhancement of inhibition is observed with *double-stranded* DNA (*7*, *13*, *19*, *26*). Dnmt1 function is modulated by RNA and DNA, both in vitro and in vivo, as first reported by Bolden and co-workers working with HeLa cell extracts (*27*). We made similar observations during the enzyme purification from MEL cells (*28*). Recent studies showed that noncoding RNA molecules regulate DNA methylation in human cells (*29*, *30*) and other organisms (*31*). Dnmt1 binds RNA polymerase II in vivo (*32*) and interacts with several RNA binding proteins (*33*).

Recent results further implicate Dnmt1 in interactions involving multiple proteins and nucleic acids (*34*−*39*). A full understanding of how Dnmt1 and other mammalian DNA cytosine methyltransferases determine and maintain the developmentally orchestrated patterns of DNA methylation demands that we understand the functional consequences of such higher order assemblies. The functional consequences of Dnmt1 forming ternary complexes involving its substrate DNA and a second nucleic acid bound at the allosteric site remain poorly understood (*10*, *13*, *15*, *22*). We investigated DNA binding at the active site and allosteric site (Figure 2) by measuring Dnmt1 processivity on its DNA substrate (*40*). We show how DNA binding at the allosteric site partially or fully inhibits the enzyme, depending on the DNA molecules that are bound at the active site and the allosteric site.

MATERIALS AND METHODS

Materials. *S*-Adenosyl-L-[methyl ^{3}H] methionine (66−82 Ci/mmol or 5900−7200 cpm/pmol), deoxy[5-^{3}H] cytidine 5′ triphosphate (19.0 Ci/mmol) ammonium salt, and Sequenase 2.0 were purchased from Amersham Corp. Poly(dI-dC) (1960 bp), poly(dG-dC) (850 bp), dITP, and dCTP were purchased from Pharmacia Biotech. DTT, Trizma, sinefungin, and activated charcoal were purchased from Sigma Chemical Co. BSA was purchased from Roche (Indianapolis, IN). BSA did not cause Dnmt1 inhibition in the concentration range from 0.2 to 0.8 mg/mL. DE81 filters were purchased from Whatman, Inc. AdoMet (85% pure) was purchased from Sigma Chemical Co. Dnmt1 was prepared from mouse erythroleukemia cells as previously described (*41*), and protein concentration was determined using pre-steady-state burst measurements as previously described and a potent oligo inhibitor (*13*, *19*). The single-stranded 30-base oligonucleotide inhibitor d(CTG GAT CCT TGC CC **^{5m}CG** CC CCT TGA ATT CCC) was prepared by solid-phase synthesis as earlier described (*13*). The methylation sequence is underlined and shown in bold. The concentrations of AdoMet, sinefungin, poly(dI-dC), poly(dG-dC), and the oligonucleotide inhibitor were determined by the absorbance at 260 nm. The respective molar absorptivity coefficients are 15.0×10^3 M^{-1} cm^{-1} for AdoMet and

sinefungin (Merck Index), 6.9×10^3 M^{-1} cm^{-1} for poly(dI-dC) bp, 8.4×10^3 M^{-1} cm^{-1} for poly(dG-dC) bp (Pharmacia technical information sheet).

Preparation of [5-^{3}H] Cytosine-poly(dG-dC) and Poly(dI-dC). ^{3}H-labeled substrates were prepared as earlier described (*42*). Briefly, the labeling reaction was prepared as 500 μM bp of poly(dI-dC) [or poly(dG-dC)] with 100 μM [5-^{3}H] dCTP, 1 mM dCTP, 10 mM dITP (or 1 mM dGTP) with 0.62 U/μL of Sequenase 2.0 in 40 mM Tris/HCl (pH 7.5), 10 mM $MgCl_2$, 50 mM NaCl, 10 mM DTT, and 1.0 mg/mL BSA. The labeling gives 13−40 cpm/pmol of base pairs for poly(dI-dC) and 60−105 cpm/pmol of base pairs for poly(dG-dC).

Preparation of Premethylated Poly(dG-dC) and Poly(dI-dC). The premethylated substrates were prepared with excess AdoMet and M·HhaI as earlier described (*19*). Briefly, M·*Hha*I (30−40 μM) and [methyl-^{14}C] AdoMet (100 μM) were incubated with 300 μM bp DNA. The labeling reaction was run for only one or two turnovers (∼1.0 min) to limit the number of methylated cytosines (^{5m}C) to the number of initially bound M·HhaI molecules. The substrates prepared by this procedure contain an average of one ^{5m}C every 7 to 20 bp, depending on the length of the labeling reaction and the ratio between total M·HhaI and DNA. All substrates prepared in this fashion showed a characteristic pre-steady-state burst (*7*, *19*) and do not show allosteric inhibition (*19*, *26*).

Preparation of [5-^{3}H] Cytosine Pm-poly(dG-dC) and Pm-poly(dI-dC). ^{3}H-labeled premethylated DNA was prepared from ^{3}H-labeled poly(dI-dC) and poly(dG-dC) using the procedure described for the preparation of unlabeled premethylated substrates.

Methylation Reactions. Incorporation of tritiated methyl groups into DNA was determined as previously described (*7*). Briefly, Dnmt1, DNA substrate, and radioactive AdoMet (15 μM) were incubated in 100 mM Tris/HCl (pH, 8.0), 10 mM EDTA, 10 mM DTT, and 0.5 mg/mL BSA at 37 °C. The enzyme and DNA concentrations are specific for each assay and described in the figure legends. The reaction was followed by placing reaction aliquots onto DE81 paper that was subsequently washed and dried.

Tritium Exchange Reactions. The tritium exchange reaction was followed essentially as previously described (*42*, *43*). Briefly, tritium exchange is measured by quenching reaction aliquots in an acid suspension of activated charcoal (HCl, pH = 2.0−2.5). The enzyme concentration, DNA concentration, and cofactor concentration are specific for each assay and described in the figure legends. All reactions were saturated with the cofactor. The reaction buffer was 100 mM Tris/HCl (pH, 8.0), 10 mM EDTA, 10 mM DTT, and 0.5 mg/mL BSA.

Data Analysis. All processivity profiles were analyzed using nonlinear regression analysis according to eqs 5 or 8 using the Levenberg−Marquardt algorithm and the nonlinear regression package in *Mathematica* (Wolfram Inc.). All linear profiles were analyzed by linear least squares using the Microcal Origin program. The results were reported as the best fit values ± standard error. Each experiment was repeated with different enzyme and substrate concentrations to test for the consistency in the observed phenomena; shown are representative examples.

RESULTS

Strategy using Chase Experiments in Studies of Processivity and Allosteric Regulation by Dnmt1 (Figures 1 and 2). In the *chase* experiments, Dnmt1 activity is measured in parallel in three different assays: *hot*, *dilute*, and *chase* (Figure 2). The hot reaction has only ^{3}H-labeled DNA (Figure 2). The dilute reaction is prepared by adding an *n*-fold excess (usually $n = 10$) of unlabeled DNA to the hot reaction aliquot with negligible changes in reaction volume. The hot and dilute reactions are started simultaneously by adding equal amounts of enzyme and the cofactor (Figure 2, prechase). The tritium release rate in the hot reaction is expected to be *n*-fold higher than in the dilute reaction because only a fraction (one *n*th) of DNA molecules in the dilute reaction are labeled. After the first few turnovers the chase reaction is prepared from the hot reaction aliquot by adding an *n*-fold excess of unlabeled DNA as in the dilute reaction (Figure 2) with negligible changes in the reaction volume. If the Dnmt1 is fully processive during the course of the measurements, adding an excess of unlabeled DNA will not affect the initial tritium release rates in the chase reaction relative to the hot reaction (Figure 2, initial post chase). If the enzyme is not processive, the tritium release rates in the chase reaction will be immediately identical to the release rates in the dilute reaction (Figure 2). For a partially processive enzyme (in which case after each turnover only a fraction of the enzyme molecules remain on the original substrate) the initial tritium release rates in the chase reaction will be between the tritium release rates for the hot and dilute reaction. The rate will gradually decrease with each turnover until the chase and dilute reactions become identical (Figure 2, final post chase). The unlabeled DNA used as the chase can be the same or different from the labeled DNA that is used as the original substrate. A combination of unlabeled and labeled DNA allows us to track which DNA binds at the active and allosteric sites (Figure 2, forms **1** → **3**). The whole process can be described quantitatively (see appendix).

We used poly(dI-dC), poly(dG-dC), and different chase substrates (*7*, *10*, *13*, *14*, *19*, *22*, *26*, *44*). Poly(dI-dC) and poly(dG-dC) substrates allow unambiguous quantitative analyses since every Dnmt1 molecule can bind the same sequence at the active site and the allosteric site (*19*). We previously showed that unmethylated poly(dI-dC) and poly(dG-dC) substrates have a maximum rate when 30−50 bp of DNA are present per Dnmt1 molecule (*7*, *13*, *14*, *19*, *44*), in which case Dnmt1 is mostly present in form **1** and partially present in form **2** (Figure 2 and ref *19*). A combination of premethylated and unmethylated substrates is attractive since the two substrate forms differ in allosteric inhibition (*19*).

Chase Experiments with ^{3}H-Poly(dI-dC) as the Substrate and Unlabeled Poly(dI-dC) as the Chase (Figure 3, Table 1). Dnmt1 shows the highest catalytic rates with poly(dI-dC) substrates and allosteric inhibition (*7*, *9*, *10*, *13*, *14*, *26*, *44*) which greatly facilitates processivity measurements. In chase experiments, the ^{3}H release reaction (Figure 1) on labeled poly(dI-dC) was challenged by a saturating concentration of unlabeled poly(dI-dC) (*19*). The hot reaction had 181 nM Dnmt1 and 10 μM bp poly(dI-dC), or 55 bp per each Dnmt1 molecule. This molar ratio gives the highest rates with poly(dI-dC) substrates, with the majority of Dnmt1

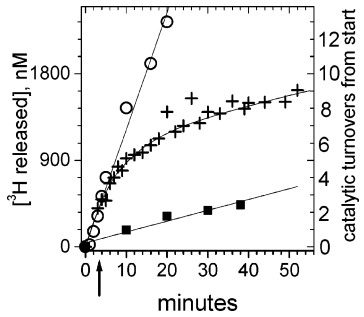

FIGURE 3: ^{3}H-poly(dI-dC) as the substrate and unlabeled poly(dI-dC) as the chase. The hot (○) reaction (10 μM bp ^{3}H-poly(dI-dC) (18 cpm/pmol) and 12.5 μM of unlabeled AdoMet) and the dilute reaction (■) were prepared from a hot reaction aliquot by adding 9-fold excess of unlabeled poly(dI-dC). Both reactions were started simultaneously by adding 181 nM Dnmt1. The chase reaction (+) was started 3 min later by mixing a hot reaction aliquot with 100 μM bp of unlabeled poly(dI-dC) (arrow). Reaction profiles were analyzed with eqs 6−8; the calculated values are summarized in Table 1.

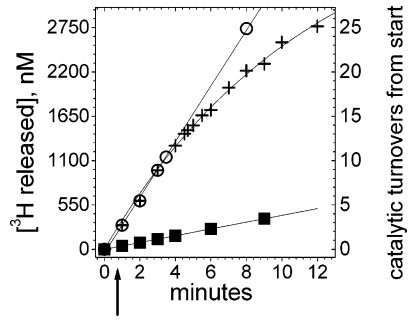

FIGURE 4: ^{3}H-pm-poly(dI-dC) as the substrate and unlabeled pm-poly(dI-dC) as the chase. The hot (○) reaction had 10 μM bp ^{3}H-pm-poly(dI-dC) (18 cpm/pmol and ^{5m}C to C ratio was 1:15) and of unlabeled AdoMet (12.5 μM). Dilute reaction (■) was prepared from a hot reaction aliquot by adding 10-fold excess of unlabeled pm-poly(dI-dC). Both reactions were started simultaneously by adding 110 nM Dnmt1. The chase reaction (+) was started 1.5 min later by adding 100 μM bp of unlabeled pm-poly(dI-dC) in the hot reaction aliquot (arrow). Profiles were analyzed using eqs 5−7; the calculated values are summarized in the Table 1.

Table 1: Processivity Rate Constants from Chase Experiments (Figures 3 and 4)[a]

	poly(dI-dC) chase with poly(dI-dC)	pm-poly(dI-dC) chase with pm-poly(dI-dC)
k_{ss}, h^{-1}	3.6 ± 0.6	not measured
CI	[2.3, 4.8]	
Ccf, (k, k_{off})	(0.46, 0.88)	
k, h^{-1}	45 ± 2	205 ± 4
CI	[40, 49]	[198, 211]
ccf, (k_{ss}, k_{off})	(0.46, 0.82)	(0.955)
k_{off}, h^{-1}	7.8 ± 0.8	5 ± 0.4
CI	[6.0, 9.0]	[4.4, 6]
ccf, (k_{ss}, k)	(0.88, 0.47)	(0.955)
p (eq 6)	0.88	0.97
$n_{1/2}$ (eq *7*)	5.5	22
hot reaction h^{-1}	43 ± 1.4	211 ± 8
dilute reaction h^{-1}	3.2 ± 0.3	25.4 ± 0.45

[a] Best fit values for turnover rates (k), substrate dissociation rates (k_{off}), and late linear phase rates (k_{ss}) were determined using eq 6. The ability of the applied equation to resolve the best fit parameters is indicated by a narrow 2σ-confidence interval (CI) and low correlation coefficient between the rates i and j (*ccf,(i,j)*). The processivity probability p was calculated according to eq 6. The "$n_{1/2}$" values (eq 7) represent a number of processive steps for the given reaction before 50% of the enzyme is dissociated of the DNA.

molecules in form **1** (Figure 2) and a smaller fraction in form **2** (*19*). The hot reaction was started by adding unlabeled AdoMet and the chase reaction was started 3 min later by adding a 9-fold excess of unlabeled poly(dI-dC) to an aliquot of the hot reaction (arrow Figure 3). The tritium release rates in the chase reaction immediately following addition of an excess of unlabeled DNA are similar to the tritium release rates in the hot reaction (Figure 3). Thus, Dnmt1 is processive on poly(dI-dC) substrate when challenged with an excess of unmethylated poly(dI-dC) (Figure 2).

The chase profiles were analyzed numerically (Table 1) to calculate the turnover rate constant (k, eq 5), the substrate DNA off rate constant (k_{off}, eq 5), and the processivity probability (eqs 6 and 7, Table 1). On the basis of this, there is an 88% chance that at the end of each catalytic turnover the next catalytic turnover will be on the same DNA molecule (eq 6, Table 1). Thus, 50% of all Dnmt1 molecules catalyze at least 5.5 turnovers on the initially bound, labeled DNA substrate before the first dissociation (eq 7, Table 1, Figure 3). The calculated rate constants are consistent with the data. The figure shows that the tritium release rate in the chase reaction becomes equal to the tritium release rate in the dilute reaction at ~24 min. Thus, 21 min after adding unlabeled DNA almost all of the Dnmt1 molecules have dissociated from the original labeled DNA substrate (Figure 2, transition **3** → **4**). The calculated half-life for dissociation of the labeled DNA from the active site is 5.3 min (Table 1), so 21 min corresponds to 4 half-lives or 94% of dissociation.

Chase Experiments with Premethylated ^{3}H-Poly(dI-dC) as the Substrate and Unlabeled Premethylated Poly(dI-dC) as the Chase (Figure 4, Table 1). Premethylated poly(dI-dC) (pm-poly(dI-dC)) has approximately one or two methylated cytosines per one Dnmt1 footprint on its DNA substrate (*19*). In comparison to unmethylated poly(dI-dC), premethylated poly(dI-dC) shows higher catalytic rates and no allosteric inhibition at high substrate concentration (*19*, *26*). In the chase experiments with tritiated pm-poly(dI-dC) (^{5m}C/C = 1/18), a 10-fold excess of unlabeled pm-poly(dI-dC) (^{5m}C/C = 1/15) was added as the chase 3 min after the start of the hot reaction (Figure 3B, arrow). The tritium release rates in the chase reaction immediately following addition of unlabeled pm-poly(dI-dC) are similar to the release rates in the hot reaction (Figure 4). Thus, Dnmt1 is processive on pm-poly(dI-dC) substrate when challenged with an excess of pm-poly(dI-dC). By numerical analysis, each catalytic turnover is followed by another turnover on the same substrate with a 95% probability and 22.8 turnovers occur before 50% of all enzyme molecules dissociate from the original substrate (eqs 5−7 and Tables 1 and 2). This high level of processivity results in the release rates never reaching the rates that were observed in the control dilute reaction. In summary, Dnmt1 is processive on pm-(dI-dC) substrate when challenged by an excess of unlabeled pm-poly(dI-dC) substrate. Also Dnmt1 is more processive on pm-poly(dI-dC) relative to poly(dI-dC) (Table 2).

Processivity Analysis with Tritiated Poly(dI-dC) as the Substrate and Unlabeled Single-Stranded Oligonucleotide Inhibitor as the Chase (Figure 5). A previously identified GC-rich 30-base-long, single-stranded oligonucleotide with a single 5-methylcytosine acts as a potent inhibitor of Dnmt1

Table 2: Processivity Rate Constants for Methylation and Exchange with Poly(dI-dC) and Poly(dG-dC) (Figures 8 and 9)

A. Methylation and ^{3}H Exchange Reaction with Poly(dI-dC) and Pm-poly(dI-dC)

	methylation with poly(dI-dC)	methylation with pm-poly(dI-dC)	methylation at high poly(dI-dC)	^{3}H exchange with sinefungin (Figure 4B)
k_{ss}, h^{-1}	6.0 ± 0.8	4.2 ± 0.4	4.2 ± 0.24	21 ± 2
CI	[4.2, 7.8]	[3.2, 5.1]	[3.7, 4.2]	[17.4, 25]
ccf (k, k_{off})	(0.14, 0.92)	(0.41, 0.87)	(0.59, 0.71)	(0.38, 0.88)
k, h^{-1}	29 ± 1	47 ± 2	20 ± 3	50 ± 5
CI	[26, 31]	[43, 50]	[19, 21]	[40, 60]
ccf (k_{ss}, k_{off})	(0.14, 0.48)	(0.41, 0.78)	(0.59, 0.84)	(0.38, 0.73)
k_{off}, h^{-1}	1.6 ± 0.2	2.8 ± 0.2	7.2 ± 0.8	2.9 ± 0.7
CI	[1.1, 2.2]	[2.3, 3.3]	[4.1, 7.7]	[1.4, 4.4]
ccf (k_{ss}, k)	(0.92, 0.48)	(0.87, 0.78)	(0.71, 0.84)	(0.88, 0.73)
p (eq 6)	0.96	0.94	0.74	0.95
$n_{1/2}$ (eq *7*)	17	11	2	14

B. Methylation and ^{3}H Exchange Reaction with Pm-poly(dG-dC)

	methylation with pm-poly(dG-dC) (Figure 8B)	exchange with sinefugin and pm-poly(dG-dC) (Figure 9 inset)
k_{ss}, h^{-1}	0.018 ± 0.010	0.2 ± 0.1
CI	[0.001, 0.022]	[0.45, 0.05]
ccf (k, k_{off})	(0.33, 0.87)	(0.06, 0.91)
k, h^{-1}	7 ± 0.2	10.5 ± 0.2
CI	[6.6, 7.2]	[10.07, 10.9]
ccf (k_{ss}, k_{off})	(0.33, 0.74)	(0.06, 0.44)
k_{off}, h^{-1}	3 ± 0.2	4.6 ± 0.3
CI	[2.4, 3.2]	[4.1, 5.5]
ccf (k_{ss}, k)	(0.87, 0.74)	(0.91, 0.44)
p (eq 6)	0.70	0.69
$n_{1/2}$ (eq 7)	1.9	1.87

[a] Best fit values for turnover rates (k), substrate dissociation rates (k_{off}), and late linear rates (k_{ss}) as indicated in the text (eq 5). All rates are given as the best fit value $\pm$ asymptotic standard error. The ability of applied equation to resolve the best fit parameters is indicated by a narrow 2σ-confidence interval (CI) and low correlation coefficient between the rates i and j (*ccf,(i,j)*). The processivity probability p was calculated according to eq 6. The "$n_{1/2}$" values (eq 7) represent a number of processive steps for the given reaction before 50% of the enzyme is dissociated of the substrate DNA.

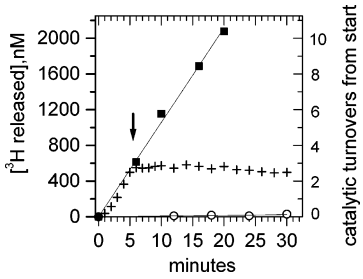

FIGURE 5: ^{3}H-poly(dI-dC) as the substrate and single-stranded oligo inhibitor as the chase. The hot (■) reaction had 10 μM bp ^{3}H-poly(dI-dC) and 12.5 μM AdoMet and 200 nM Dnmt1. Dilute reaction (○) was prepared from a hot reaction aliquot by adding 250 nM of the single-stranded inhibitor. The chase reaction (+) was started 5 min after the hot and dilute reactions by adding 250 nM of the oligo inhibitor in a hot reaction aliquot. Measured ^{3}H release rate constants are 46 ± 0.8 h^{-1} for the hot reaction, while the dilute reaction was at the background level. The chase reaction profile clearly shows complete Dnmt1 inhibition immediately following addition of the oligo inhibitor.

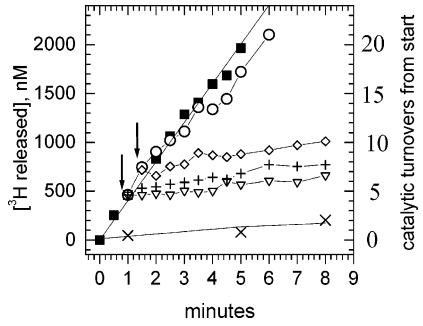

FIGURE 6: ^{3}H-pm-poly(dI-dC) as the substrate and unlabeled poly(dI-dC), poly(dG-dC), pm-poly(dG-dC), and poly(dA-dT) as the chase. The hot (■) reaction had 10 μM bp ^{3}H-pm-poly(dI-dC), 12.5 μM AdoMet, and 90 nM Dnmt1. The chase reaction was started 1 to 1.5 min after the hot reaction by adding to a hot reaction aliquot: 100 μM bp of cold poly(dI-dC) (▽), 100 μM bp of cold poly(dG-dC) (+), 100 μM bp of cold poly(dA-dT) (◇), or 100 μM bp of pm-poly(dG-dC) (○). For clarity, only the dilute reaction (×) with poly(dI-dC) is shown.

($K_i \sim 30$ nM), and DNA methylation in vivo (*13*). This inhibitor appears to bind to the allosteric site through the formation of an inhibitory ternary complex (enzyme/substrate/inhibitor) (*13*). Here we used chase experiments to further define this inhibitor's mechanism of action. The hot reaction was prepared using 200 nM Dnmt1 and 10 μM bp tritiated poly(dI-dC), or 50 bp per one Dnmt1 molecule, in which case Dnmt1 is largely in form **1** (Figure 2), and a small fraction is in form **2** (Figure 2). The hot reaction was started by adding unlabeled AdoMet (12.5 μM), and 5 min later (arrow Figure 5), the chase reaction was started by adding a saturating concentration (250 nM) of the inhibitor as the chase. Interestingly, adding the inhibitor led to the immediate cessation of catalysis (Figure 6), in contrast to the delayed impact observed with excess poly(dI-dC) as the chase (Figure 3). This instant inhibition of processive catalysis must be caused by the formation of the ternary complex (enzyme/substrate/inhibitor) (Figure 2, form **3**), since Dnmt1 is processive on poly(dI-dC) substrate (Figure 3, Table 1, $k_{off} = 7.8 \pm 0.8$ h^{-1}) and its active site is not readily available

for interaction with DNA that was added as the chase (Figure 2., transition **1** → **4**).

In summary, we found that the allosteric site on Dnmt1 can bind a second DNA molecule when the active site is involved in processive catalysis (Figure 2, transition **1** → **3**). The difference between the chase reaction with poly(dI-dC) (Figure 3) and inhibitor (Figure 5) indicates how different DNA molecules can lead to full or partial inhibition of catalytic activity. Finally, the chase experiments confirm the original proposal (*13*) that the potent Dnmt1 inhibitor binds allosterically through the formation of a ternary complex (enzyme/substrate/inhibitor) (Figure 2, form **3**).

Processivity Analysis with ^{3}H-pm-poly(dI-dC) as the Substrate and Unlabeled Poly(dI-dC), Poly(dG-dC), Pm-poly(dG-dC), and Poly(dA-dT) as the Chase (Figure 6). We used chase experiments to test how unmethylated DNA affects the catalytic activity on premethylated DNA. In comparison to premethylated DNA, unmethylated DNA led to Dnmt1 inhibition at the high substrate concentration that is associated with allosteric site (*7*, *10*, *13*, *14*, *19*, *22*, *26*, *44*). Here we use the chase experiments to analyze how saturation with unmethylated poly(dG-dC), poly(dI-dC), and premethylated poly(dG-dC) impact Dnmt1's processive catalysis with pm-poly(dI-dC) (Figure 6). Since Dnmt1 is processive with ^{3}H-pm-poly(dI-dC) (Figure 4, Table 1, $k_{off} = 5 \pm 0.4$ h^{-1}), its active site is not readily accessible for interaction with chase molecules.

The hot reaction was prepared by incubating 90 nM Dnmt1 with 10 μM bp ^{3}H-pm-poly(dI-dC) (110 bp per each Dnmt1 molecule); thus, there is an excess of ^{3}H-pm-poly(dI-dC) relative to Dnmt1 (Figure 2), and both the active and the allosteric sites have access to DNA (Figure 2, form **2**) (*19*). Hot and dilute reactions were started simultaneously by adding unlabeled AdoMet (12.5 μM). The chase reaction was initiated 30−45 s after the start of the hot reaction by adding 100 μM bp poly(dI-dC), poly(dG-dC), or pm-poly(dG-dC) to separate aliquots of the hot reaction. The slope of the chase reaction immediately following the addition of unlabeled poly(dI-dC) and poly(dG-dC) is identical to the slope in dilute reaction (Figure 3B). Thus, by forming a heterocomplex (Figure 2, form **3**) unmethylated poly(dI-dC) interrupts processive catalysis on premethylated ^{3}H-poly(dI-dC) but not on unmethylated ^{3}H-poly(dI-dC) (Figure 3). In contrast, premethylated poly(dG-dC) and poly(dI-dC) do not interrupt processive catalysis on ^{3}H-pm-poly(dI-dC) (Figures 4 and 6).

A recent study showed that Dnmt1 is inhibited by poly(ADP-ribose) in vivo as a part of the poly(ADP-ribose)-polymerase-1 (PARP-1) response to DNA damage (*45*). This provides a plausible explanation for the previous surprising observation that Dnmt1 is inhibited by poly(dA)-poly(dT) and poly(dA-dT) (*27*). In Figure 6, we show that saturation with poly(dA-dT) stops Dnmt1's processive catalysis on pm-poly(dI-dC) by binding at the allosteric site (Figure 2., transition **1** → **3**)

Chase Experiments with Premethylated ^{3}H-poly(dG-dC) as the Substrate and Unlabeled Premethylated Poly(dG-dC) as the Chase (Figure 7, Table 1). Dnmt1 has exceptionally slow catalytic rates with DNA molecules that have CpG target sites (*19*). We wanted to analyze how slow turnover rates are affected by Dnmt1−DNA interactions. With pm-poly(dG-dC), the hot reaction was prepared as ^{3}H-pm-poly(dG-dC) (8 μM bp, 88 cpm/pmol, ratio ^{5m}C:C 1 to 14). The dilute reaction was prepared from a hot reaction aliquot by adding unlabeled pm-poly(dG-dC) (80 μM bp, ratio ^{5m}C:C 1 to 12). Both reactions were started simultaneously by adding Dnmt1 (85 nM) and 15 μM of unlabeled AdoMet. The hot and dilute reaction profiles were analyzed using a linear equation and the best fit rates were 11.3 ± 0.8 h^{-1} and 1.0 ± 0.04 h^{-1}, respectively. The chase reaction was started 5 min later (approximately at the end of the first turnover) by mixing a hot reaction aliquot with 80 μM of unlabeled pm-poly(dG-dC). The slow rates with the two poly(dG-dC) substrates preclude measuring of Dnmt1 processivity in multiple turnovers as with poly(dI-dC) substrates.

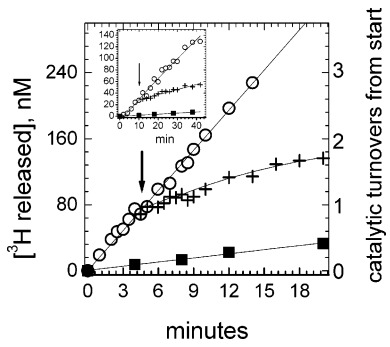

FIGURE 7: ^{3}H-pm-poly(dG-dC) as the substrate and unlabeled pm-poly(dG-dC) as the chase. Inset, ^{3}H-poly(dG-dC) as substrate and unlabeled poly(dG-dC) as the chase. The hot (○) reaction had 10 μM bp ^{3}H-pm-poly(dG-dC) and 12.5 μM of unlabeled AdoMet. Dilute reaction (■) was prepared from a hot reaction aliquot by adding 10-fold excess of unlabeled pm-poly(dG-dC). Both reactions were started simultaneously by adding 85 nM Dnmt1. The chase reaction (+) was started at the start of the second turnover (5 min) by adding 80 μM bp of cold pm-poly(dG-dC) to an aliquot of the hot reaction. The inset shows a chase experiment with ^{3}H-poly(dG-dC) as substrate and cold poly(dG-dC) as the chase. The hot reaction (○) was prepared as 8 μM bp of ^{3}H−GdC (102 cpm/pmol), 15 μM of unlabeled AdoMet, and 200 nM Dnmt1. Dilute reaction (■) was prepared from a hot reaction aliquot by adding 10-fold excess of unlabeled pm-poly(dG-dC). The chase reaction (+) was started 15 min after the start of the hot reaction arrow by adding 80 μM bp of cold poly(dG-dC) to the hot reaction aliquot.

The decay in tritium release following the addition of the unlabeled chase was analyzed using the exponential decay equation ([^{3}H released] = $A(1 - e^{-kt}) + pt$); The tritium release rate constant (k) immediately following the start of the chase reaction is equal to 5 ± 0.9 h^{-1}, The ratio between the initial chase and dilute rates is about 46% of the ratio between hot and dilute rates (Table 2B). Thus, addition of the unlabeled chase results in ~46% retention of Dnmt1 on the original labeled DNA (Figure 2, transition **1** → **3**). The lower processivity with pm-poly(dG-dC) relative to pm-poly(dI-dC) can be attributed to lower turnover rates (eq 6), rather than the difference in DNA binding at the allosteric site, because pm-poly(dG-dC) cannot displace Dnmt1 in processive catalysis on pm-poly(dI-dC) (Figure 6).

Dnmt1 catalytic rates with poly(dG-dC) (inset, Figure 7) are even slower than with pm-poly(dG-dC) and consistent with rates measured with other unmethylated substrates (*7*, *9*, *11*, *44*). It takes about an hour to finish the first turnover and about 3−4 h to finish the second turnover. Thus, we used the chase experiments to analyze the enzyme's commitment for a given DNA substrate during its slow first catalytic turnover (Figure 2). The hot reaction was prepared

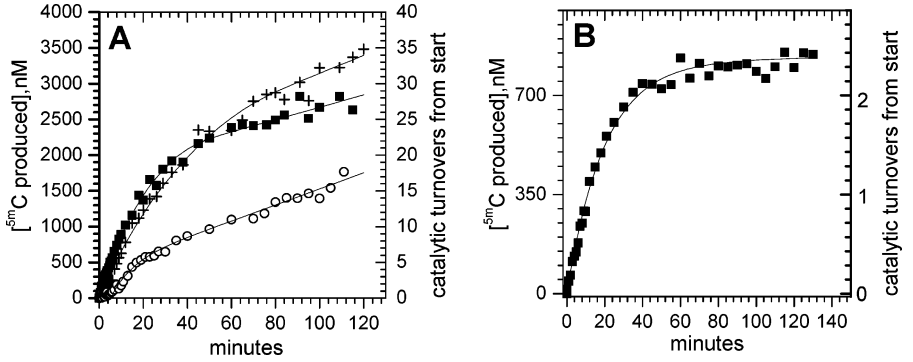

FIGURE 8: (A, B) Dnmt1 methylation reaction with poly(dI-dC) (A, 12 μM and 260 μM), pm-poly(dI-dC), and methylation reaction with pm-poly(dG-dC) (B). (A) Dnmt1 methylation reaction with 12 μM bp (+) poly(dI-dC), 260 μM bp (○) poly(dI-dC), and 12 μM pm-poly(dI-dC) (■). All three assays had 125 nM Dnmt1 and 12.5 μM [^{3}H methyl] AdoMet (6750 cpm/pmol). All profiles were analyzed using eqs 8, 6, and 7 (Table 2A). Both poly(dI-dC) and pm-poly(dI-dC) were 1960-bp-long, pm-poly(dI-dC) with one in eight cytosines methylated. (B) Analysis of processivity in Dnmt1 (300 nM) methylation reaction with 12 μM bp (■) pm-poly(dG-dC) and 12.5 μM [^{3}H methyl] AdoMet (6750 cpm/pmol). The profile was analyzed using eqs 8, 6, and 7 (Table 2B).

using 8 μM bp of ^{3}H-poly(dG-dC) (102 cpm/pmol), 15 μM of unlabeled AdoMet, and 200 nM Dnmt1 (40 bp per one Dnmt1 molecule). The dilute reaction was prepared from the hot reaction aliquot by adding 144 μM bp of unlabeled poly(dG-dC). The chase reaction was started 15 min after the start of the hot reaction (at the end of the initial lag; *19*) by adding 144 μM bp of unlabeled poly(dG-dC) to a hot reaction aliquot. The best fit rate constant was 1 ± 0.11 h^{-1} for the hot reaction, 0.06 ± 0.005 h^{-1} for the dilute reaction, and 0.27 ± 0.003 h^{-1} for the chase reaction. The ratio between the chase and dilute reaction rates is 25% of the ratio between the rates measured in the hot and dilute reactions. Thus, at least 75% of the initially bound Dnmt1 can be readily displaced from the poly(dG-dC) (Figure 2, transition **3** → **4**). This indicates that during the slow turnover the majority of Dnmt1 molecules are not committed to the initially bound substrate (*19*). This is consistent with our earlier study which showed that slow turnover with unmethylated substrates can be attributed to slow formation of early reaction intermediates leading to target base attack (*19*). Interestingly, the chase experiments showed that Dnmt1 can be readily displaced from poly(dG-dC) substrates but not from poly(dI-dC) substrates, in contrast to the bacterial enzyme M·HhaI (*42*).

Dnmt1 Processivity Analysis by Following Methylation (Figure 8 A,B and Figure 9). Dnmt1 reactions often show a gradual decrease in the initial linear profile followed by the late linear phase, as seen in the methylation reaction with poly(dI-dC), pm-poly(dI-dC) (Figure 8A), pm-poly(dG-dC) (Figure 8B), and in the ^{3}H exchange reaction (Figure 1) with sinefungin and poly(dI-dC) or pm-poly(dG-dC) (Figure 9). Interestingly, the high substrate concentrations that lead to allosteric inhibition also lead to changes in this biphasic profile (Figure 8A). We suggest that this biphasic reaction profile is caused by Dnmt1's processivity. Alternative explanations such as product inhibition, substrate depletion, or enzyme instability with time are unlikely. The observed biphasic profiles (Figures 8 and 9) cannot be attributed to products of the methylation reaction ^{5m}C or AdoHcy since we observe similar profiles when following the exchange reaction with sinefungin (Figure 9). The exchange reaction has no "chemical" product; the reaction is only replacing ^{3}H with H at the cytosine carbon 5 (Figure 1). Also, the reaction at high poly(dI-dC) concentration shows an early

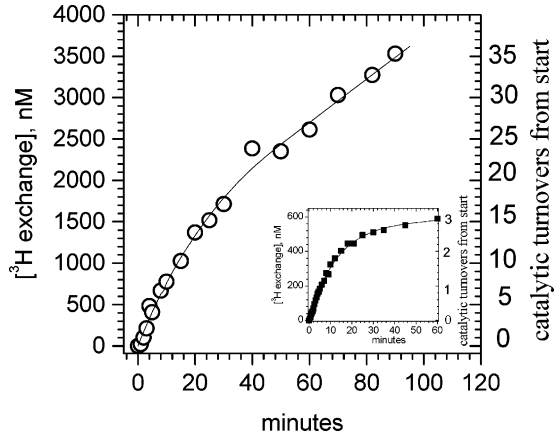

FIGURE 9: ^{3}H exchange reaction with sinefungin and ^{3}H-poly(dI-dC) and ^{3}H-pm-poly(dG-dC) (inset). ^{3}H exchange reaction (○) with 95 nM Dnmt1 20 μM sinefungin and 10 μM bp of ^{3}H-poly(dI-dC) (18 cpm/pmol). The inset shows processivity profiles with sinefungin and ^{3}H-pm-poly(dG-dC) (106 cpm/pmol), using 70 nM Dnmt1. The reaction profiles were analyzed using eqs 8, 6, and 7, and the calculated values are given in the Table 2.

transition to the late linear phase even though less product is being generated. The biphasic reaction profiles are also not due to substrate depletion since the late linear profile is observed earlier at the higher concentration of poly(dI-dC). Finally, the biphasic reaction profiles are not due to enzyme instability since all reactions were measured in the same conditions (often in parallel) and the shape of each reaction profile depends on the substrate type and the substrate concentration.

We suggest that Dnmt1's processive catalysis accounts for the biphasic reaction profiles (Figures 8 and 9). Processive catalysis requires that the dissociation rate for the substrate DNA is slower than the turnover rate (see appendix). These conditions are well-known to lead to a pre-steady-state burst with DNA substrates that have only one methylation site (*7*). However, with substrates that have multiple methylation sites, only a fraction of substrate DNA will dissociate after each turnover during processive catalysis. All enzyme molecules will be initially DNA bound at the start of the first turnover. Since the enzyme is not 100% processive, at the start of the second turnover a fraction of enzyme molecules will go through a slow dissociation step, while the rest will go directly to the next turnover on the same

DNA. With each subsequent turnover, this partitioning results in a gradual rate decrease that is proportional to the fraction of enzyme molecules which enter the slow dissociation step. The partitioning is repeated with each turnover until the catalytic contribution from enzyme molecules retained on the initial DNA is equal to the catalytic contribution from enzyme molecules that are reassociating. At that point a quasi steady state is established, and the reaction profile shows the late linear phase. Consistent with this scenario, pm-poly(dG-dC) shows both poor processivity (Figure 7) and an earlier onset of the late linear phase than poly(dI-dC) and pm-poly(dI-dC) (Figures 3 and 4).

We have analyzed these biphasic reaction profiles numerically to calculate the turnover rate constant k (eq 5, Table 2), the Dnmt1−DNA off rate constant k_{off} (eq 5, Table 2), and the processivity probability (eqs 6 and 7, Table 2). We find that the allosteric inhibition by excess unmethylated poly(dI-dC) (Figure 8A) is caused by a decrease in processivity (Table 2) as a result of an increase in the Dnmt1−DNA off rate constant (Table 2) and a decrease in the catalytic rate constant (Table 2). When Dnmt1 is partially saturated with poly(dI-dC) and substrate inhibition is not present to the full extent, poly(dI-dC) and pm-poly(dI-dC) show similar processivity probabilities (Table 2, eq 6). This similarity is a result of a compensatory difference in the turnover rates (k) and off rates (Table 2). The calculated turnover constants (k, Table 2) from the processivity measurements in the methylation reaction are lower than the turnover constants calculated from the chase processivity experiments (k, Table 1). The difference is due to the earlier described (*19*) discrepancy between ^{3}H release and methylation rates with poly(dI-dC) substrates. The calculated processivity in the methylation reaction (Table 2 and Figure 8A) and in the exchange reaction with sinefungin (Table 2, Figure 9) are similar due to similar turnover rates. Also, due to slower turnover rates, pm-poly(dG-dC) substrates show less processivity in methylation (Figure 8B) and the exchange reaction (Figure 9, inset) relative to poly(dI-dC) and pm-poly(dI-dC) substrates.

DISCUSSION

Dnmt1 has at least two DNA binding sites, the active site and the allosteric site (*10*). Here we use chase experiments (Figure 2) to study the ternary complexes between Dnmt1 and DNA bound at the active and the allosteric sites. In chase experiments an ongoing ^{3}H release/exchange reaction (Figure 1) on a ^{3}H-labeled DNA is challenged with an excess of unlabeled DNA (Figure 2), allowing the tracking of which DNA molecule acts as a substrate and which acts as an allosteric regulator (Figure 2, transition **1** → **3** → **4**). The chase experiments (Figures 6 and 7) support proposals (*13*) that the two sites on Dnmt1 can independently bind two different DNA molecules (trans mechanism) (Figure 10). Alternatively, DNA binding at the active site directly leads to binding of *adjacent* DNA sites at the allosteric site (cis mechanism). We also show that the allosteric site is open for interaction with different DNA molecules that can regulate the ongoing catalytic activity at the active site (Figures 5 and 6). Our results provide a basis for understanding how DNA sequence, methylation status, and structure regulate Dnmt1's allosteric inhibition and processive catalysis. In the next few paragraphs, we integrate results from this study with the results from other Dnmt1 studies to provide our current view of allosteric regulation of Dnmt1 (Figure 10B).

The partial inhibition observed with excess unmethylated DNA is often shown in the literature (*9*, *13*, *19*, *22*, *44*). Here we show such inhibition can be due to a decrease in the turnover rate constant and an increase in the substrate DNA off rate (Table 2), both of which can lead to lower processivity (eq 6 and Figure 8A). Interestingly, Dnmt1 undergoes a slow conformational change from an inactive to active form at the start of catalysis on unmethylated DNA (Figure 10B), which can be triggered by cofactor binding and possibly by DNA release from the allosteric site (*19*).

Studies of a Dnmt1 mutant lacking the functional N terminal domain indicate that some form of allosteric inhibition is present even with premethylated substrates (*10*). However, there is no evidence that such inhibition results from DNA binding at both the active and the allosteric sites (*13*, *19*, *26*, *44*). Here we show that unmethylated DNA, but not premethylated DNA, interferes with processive catalysis on premethylated DNA (Figures 4 and 6). This observation may help explain why previous studies showed that Dnmt1 is not self-activated by ^{5m}C produced during the initial stages of methylation (*19*). The higher methylation rates with premethylated DNA are only observed in the absence of significant stretches of unmethylated DNA which can cause allosteric inhibition (Figure 10B). Such conditions are seen when at least one methylcytosine lies within one enzyme footprint, independent of the distance between the methylcytosine and the target cytosine (*11*, *19*). Allosteric activation with premethylated substrates is unlikely (*19*).

We previously described a GC-rich single-stranded oligonucleotide with one ^{5m}C site as a potent Dnmt1 inhibitor (K_i ∼ 30 nM), which binds at the allosteric site and reverses DNA methylation in cells (*13*). We found that the single-stranded oligo inhibitor completely stops the ongoing processive catalysis on unmethylated DNA (Figure 5). This is in contrast to double-stranded unmethylated poly(dI-dC) and poly(dG-dC), which show only a partial inhibition of enzyme activity (*13*, *26*, *44*) and processive catalysis in the same conditions (Figure 8A). Interestingly, in contrast to double-stranded DNA, preexisting methylation leads to more potent inhibition with the single-stranded DNA inhibitor (*13*).

Dnmt1 functions within replication forks (*23*, *37*, *39*, *46*) and chromatin remodeling complexes (*47*). Dnmt1 interactions with other proteins may affect its processivity by altering its turnover rate and substrate DNA off rate (eq 6). It seems likely that the two independent DNA binding sites on Dnmt1 and the mechanism present in Figure 10 are also present in vivo. Although which regulatory sequences might bind the allosteric site in vivo are currently unknown, mounting evidence indicates that DNA methylation can be controlled by noncoding RNA molecules (*27*−*31*) and poly(ADP-ribose) (*45*). Twenty years ago, Bolden and coworkers suggested that RNA could regulate Dnmt1 and DNA methylation in vivo (*27*). The authors found that Dnmt1 is inhibited in HeLa cells extract by RNA; further, the inhibition potency depends on the sequence, including the surprising discovery that Dnmt1 is inhibited by poly(dA)-poly(dT) and poly(dA-dT). Subsequent studies also reported Dnmt1 inhibition by RNA molecules (*28*) and showed that Dnmt1 interacts with RNA polymerase II in vivo (*32*) and with several RNA

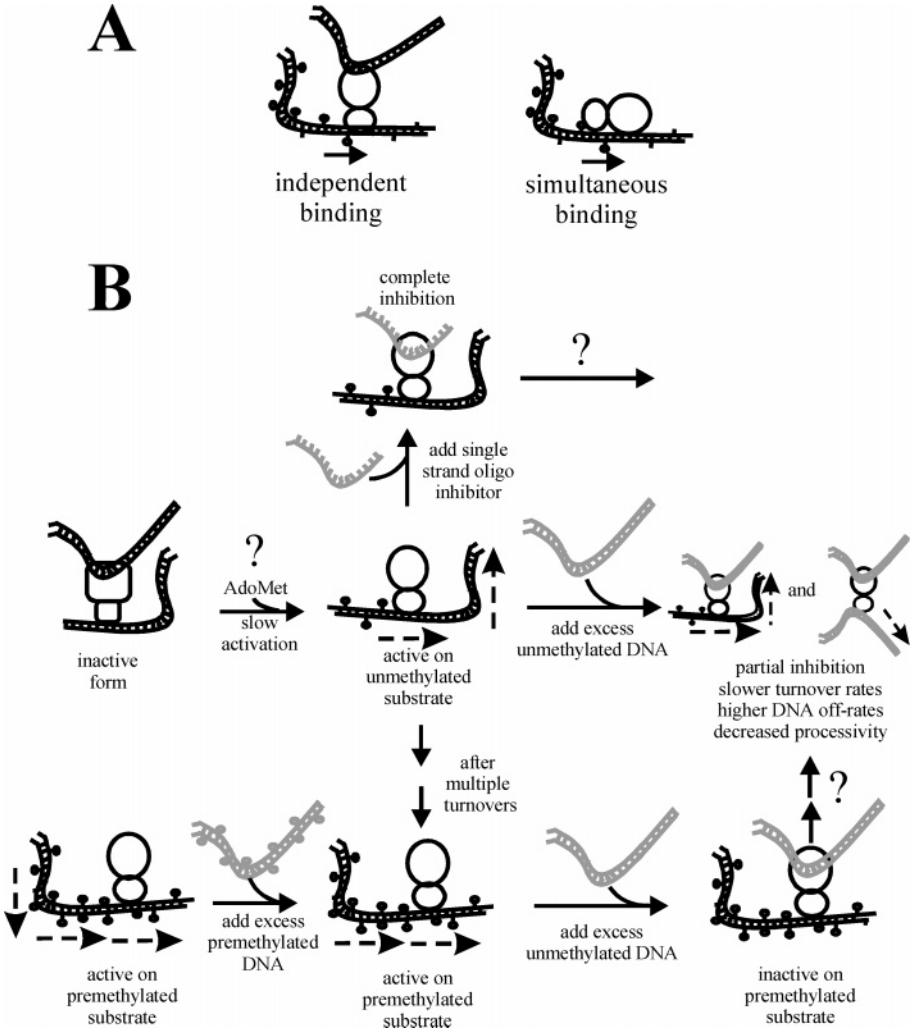

FIGURE 10: (A, B) Allosteric regulation of Dnmt1 (ovals, small catalytic domain and the large regulatory domain) with different DNA molecules. (A) Two modes for allosteric regulation of Dnmt1, DNA binding at the active site leads directly to binding of the adjacent DNA sites at the allosteric site (cis binding), or the active site and the allosteric site can bind DNA independently (trans binding). (B) With unmethylated DNA, DNA binding at the allosteric site can cause slow transition from the inactive to the active form following AdoMet binding and the start of catalysis (*19*). During the catalytic cycle, the active site can be involved in catalysis, while the allosteric site is accessible to bind "regulatory" DNA. Binding of the single-stranded DNA inhibitor (*13*) leads to a complete inhibition, and binding of unmethylated DNA results in higher off rates, lower turnover rates, and ultimately lower processivity. With premethylated DNA substrates, binding of premethylated DNA at the allosteric site does not alter the enzyme's activity, while binding of unmethylated DNA leads to a stop in catalytic activity. The question marks indicate steps for which the mechanism is not fully understood.

binding proteins (*33*). These RNA molecules are likely to modulate or completely inhibit the catalytic activity of Dnmt1 by binding at the allosteric site and by forming a ternary complex (Figure 10B). Such inhibition could depend on RNA sequence, methylation, and structure (i.e., double stranded vs single stranded) as suggested in Figure 10B.

In general, Dnmt1's processivity is determined by its catalytic turnover rate and dissociation rate from the DNA (see appendix, eq 6). Thus, lower turnover rates can account for lower processivity with poly(dG-dC) relative to poly(dI-dC) or lower processivity with unmethylated DNA relative to premethylated DNA. Because the rates with poly(dG-dC) are similar to the rates measured with other unmethylated substrates with CG target sites (*9*, *19*, *40*, *44*), we suggest that previous reports on the lack of processivity with unmethylated DNA substrates can be attributed to the slow turnover rates and a lack of multiple turnovers (*40*, *48*). The catalytic rates measured with pm-poly(dG-dC) are also comparable to the catalytic rates measured with other premethylated substrates with CG target sites (*9*, *19*, *40*, *44*). However, despite similar rates, different premethylated substrates show different catalytic features (*9*, *10*, *40*), which in part could depend on the methylation pattern and the sequence surrounding the target site. Such differences account for the differences in processivity between different premethylated substrates (*40*) including pm-poly(dG-dC) (*19*).

ACKNOWLEDGMENT

We wish to thank Mr. Jamie Witham for help with these measurements. We are grateful to Dr. D. J. T. Porter from Glaxco Welcome for his generous advice in deriving the processivity equation. We are grateful to Dr. Jim Flynn for his expert advice and excellent discussions. Thanks to Dr. Peter Vollmayr and Dr. Ana M. Ojeda for their efforts in purification of Dnmt1. We are grateful to R. August Estabrook and Dr. Matthew Purdy for their insightful comments on the text of the manuscript.

APPENDIX: ANALYTICAL DESCRIPTION OF PROCESSIVE CATALYSIS BY DNA METHYLTRANSFERASES

Analysis of Processivity Data. The mathematical model is an adaptation of similar models used to describe processivity of DNA helicase (*49*, *50*) or the kinetics of polymer growth in polymer chemistry (*51*). The processivity of a methyltransferase can be schematically described as

$$\begin{array}{ccccccccc} ES_0 & \xrightarrow{k} & EP_1 & \xrightarrow{k} & EP_2 & \xrightarrow{k} & .. & \xrightarrow{k} & EP_i \xrightarrow{k} .. \\ & & \downarrow k_{off} & & \downarrow k_{off} & & & & \downarrow k_{off} \end{array}$$

Every k is a turnover rate constant for a particular catalytic step (e.g., methylation or ^3H release), and every k_{off} is dissociation rate constant for enzyme−DNA complex. EP_i represents the enzyme that has processed i steps, and ES_o is the initial enzyme−DNA complex. ES_o is equal to the total enzyme concentration in the assay if the enzyme and the DNA concentration are well above dissociation constant for the enzyme−DNA complex. The scheme assumes that ^3H release and the methylation reaction are irreversible as previously shown (*43*). The concentration of EP_i as a function of time can be described with a differential equation:

$$\frac{d[EP_i]}{dt} = k[EP_{i-1}] - (k + k_{off})[EP_i] \quad (1)$$

Equation 1 can be integrated starting from the initial ES_o complex to give the expression that describes the concentration of every EP_i species as a function of time:

$$[EP_i](t) = \frac{k^i t^{i-1}}{t!}[ES_o]e^{-(k+k_{off})t} \quad (2)$$

The product formed in the processive step i by EP_{i-1} can be calculated as

$$\frac{d[P_i]}{dt} = k[EP_{i-1}] \quad (3)$$

Equation 3 is combined with eq 2 and integrated to give the expression for the product formed in the processive step i:

$$[P_i] = [ES_o]\frac{k^i}{(k + k_{off})^i}\left(1 - e^{-(k+k_{off})t} - e^{-(k+k_{off})t}\sum_{l=1}^{i-1}\frac{(k + k_{off})^l t^l}{l!}\right) \quad (4)$$

The final equation for the product formed in a processive reaction is a sum of all processive steps ($i = 1$ to n) and equal to

$$[P] = (\sum_{i=1}^{n} P_i) \quad (5)$$

Equation 5 is an asymptotic function with the asymptote parallel to x axis and equal to

$$\lim_{n\to\infty} \sum_n [ES_o]p^n$$

where n is the number of the processive steps and p is the processivity probability defined as

$$p = \frac{k}{k + k_{off}} \quad (6)$$

The probability for the processive step n is equal to

$$p_n = \left(\frac{k}{k + k_{off}}\right)^n \quad (7)$$

Theoretically n is equal to infinity. In our experience, for all practical purposes the precision of best fit values will not significantly increase once n reaches the values that give a processivity probability of 0.05 or below (eq 7), i.e., 95% of enzyme molecules have dissociated from the original substrate. Equation 5 describes *the first processive cycle*, which includes catalytic turnovers from all Dnmt1 molecules before their first dissociation from the initial DNA substrate.

The main part of our processivity profiles come from the first processive cycle (i.e., Figure 4); however, in some measurements the late linear part and the subsequent processive cycles are substantial (i.e., Figure 3). Accordingly, the experimental processivity profiles show a late linear phase that does not end with an asymptote parallel to the x axis as predicted by the eq 5. Developing a mathematical model that describes multiple processive cycles as a function of k and k_{off} is impractical. Accordingly, we describe the late linear part empirically by adding a second linear factor to the eq 5:

$$[P] = (\sum_{i=1}^{n} P_i) + k_{ss}[ES_o]t \quad (8)$$

The first part of the eq 8 comes from eq 5 and represents the analytic description of the first processive cycle. The second part in eq 8 is the late linear phase that represents multiple processive cycles. The k_{ss} is an empirical rate constant that describes the catalytic rate in the late linear phase, while the $[ES_o]t$ factor indicates that the late linear phase is proportional to the total enzyme concentration and linear with time.

The selection between eqs 5 or 8 is empirical. We analyzed each profile using both equations, and the fit quality for each case was compared. When profiles with no late linear phase are analyzed using eq 8, the fit gives large errors for k_{ss}, and (or) k_{ss} takes nonsense values such as $k_{ss} < 0$, and (or) k_{ss} becomes highly correlated with k_{off}, all indicating that eq 5 is a better choice for such cases. The experimental profiles can be directly analyzed using eq 5 or 8 with all three parameters (k, k_{off}, k_{ss}) set as the free variables. ES_o is poorly resolved as the free parameter (i.e., high correlation to k value) using eqs 5 or 8, so in all fits we kept ES_o constant according to the value calculated from other measurements. All fits converge easily even when the initial values for the

fit parameters are given borderline reasonable estimates (Tables 1 and 2).

REFERENCES

1. Jones, P. A., and Takai, D. (2001) The role of DNA methylation in mammalian epigenetics, *Science 293*, 1068−1070.
2. Robertson, K. D., and Jones, P. A. (2000) DNA methylation: past, present and future directions, *Carcinogenesis 21*, 461−467.
3. Egger, G., Liang, G., Aparicio, A., and Jones, P. A. (2004) Epigenetics in human disease and prospects for epigenetic therapy, *Nature 429*, 457−463.
4. Pradhan, S., and Esteve, P. O. (2003) Mammalian DNA (cytosine-5) methyltransferases and their expression, *Clin. Immunol. 109*, 6−16.
5. Xie, S., Wang, Z., Okano, M., Nogami, M., Li, Y., He, W. W., Okumura, K., and Li, E. (1999) Cloning, expression and chromosome locations of the human DNMT3 gene family, *Gene 236*, 87−95.
6. Okano, M., Xie, S., and Li, E. (1998) Dnmt2 is not required for de novo and maintenance methylation of viral DNA in embryonic stem cells, *Nucleic Acids Res. 26*, 2536−2540.
7. Flynn, J., Glickman, J. F., and Reich, N. O. (1996) Murine DNA cytosine-C5 methyltransferase: pre-steady- and steady-state kinetic analysis with regulatory DNA sequences, *Biochemistry 35*, 7308−7315.
8. Yokochi, T., and Robertson, K. D. (2002) Preferential methylation of unmethylated DNA by Mammalian de novo DNA methyltransferase Dnmt3a, *J. Biol. Chem. 277*, 11735−11745.
9. Bacolla, A., Pradhan, S., Roberts, R. J., and Wells, R. D. (1999) Recombinant human DNA (cytosine-5) methyltransferase. II. Steady-state kinetics reveal allosteric activation by methylated DNA, *J. Biol. Chem. 274*, 33011−33019.
10. Bacolla, A., Pradhan, S., Larson, J. E., Roberts, R. J., and Wells, R. D. (2001) Recombinant human DNA (cytosine-5) methyltransferase. III. Allosteric control, reaction order, and influence of plasmid topology and triplet repeat length on methylation of the fragile X CGG•CCG sequence, *J. Biol. Chem. 276*, 18605−18613.
11. Aubol, B. E., and Reich, N. O. (2003) Murine DNA cytosine C(5)-methyltransferase: in vitro studies of de novo methylation spreading, *Biochem Biophys. Res. Commun. 310*, 209−214.
12. Flynn, J., Azzam, R., and Reich, N. (1998) DNA binding discrimination of the murine DNA cytosine-C5 methyltransferase, *J. Mol. Biol. 279*, 101−116.
13. Flynn, J., Fang, J. Y., Mikovits, J. A., and Reich, N. O. (2003) A potent cell-active allosteric inhibitor of murine DNA cytosine C5 methyltransferase, *J. Biol. Chem. 278*, 8238−8243.
14. Flynn, J., and Reich, N. (1998) Murine DNA (cytosine-5-)-methyltransferase: steady-state and substrate trapping analyses of the kinetic mechanism, *Biochemistry 37*, 15162−15169.
15. Pradhan, S., and Esteve, P. O. (2003) Allosteric activator domain of maintenance human DNA (cytosine-5) methyltransferase and its role in methylation spreading, *Biochemistry 42*, 5321−5332.
16. Pradhan, S., and Roberts, R. J. (2000) Hybrid mouse-prokaryotic DNA (cytosine-5) methyltransferases retain the specificity of the parental C-terminal domain, *EMBO J. 19*, 2103−2114.
17. Lauster, R., Trautner, T. A., and Noyer-Weidner, M. (1989) Cytosine-specific type II DNA methyltransferases. A conserved enzyme core with variable target-recognizing domains, *J. Mol. Biol. 206*, 305−312.
18. Yoder, J. A., Soman, N. S., Verdine, G. L., and Bestor, T. H. (1997) DNA (cytosine-5)-methyltransferases in mouse cells and tissues. Studies with a mechanism-based probe, *J. Mol. Biol. 270*, 385−395.
19. Svedruzic, Z. M., and Reich, N. O. (2005) DNA Cytosine c(5) methyltransferase Dnmt1: catalysis-dependent release of allosteric inhibition, *Biochemistry 44*, 9472−9485.
20. Ivanetich, K. M., and Santi, D. V. (1992) 5,6-dihydropyrimidine adducts in the reactions and interactions of pyrimidines with proteins, *Prog. Nucleic Acid Res. Mol. Biol. 42*, 127−156.
21. Araujo, F. D., Croteau, S., Slack, A. D., Milutinovic, S., Bigey, P., Price, G. B., Zannis-Hajopoulos, M., and Szyf, M. (2001) The DNMT1 target recognition domain resides in the N terminus, *J. Biol. Chem. 276*, 6930−6936.
22. Bestor, T. H. (1992) Activation of mammalian DNA methyltransferase by cleavage of a Zn binding regulatory domain, *EMBO J. 11*, 2611−2617.
23. Chuang, L. S., Ian, H. I., Koh, T. W., Ng, H. H., Xu, G., and Li, B. F. (1997) Human DNA-(cytosine-5) methyltransferase-PCNA complex as a target for p21WAF1, *Science 277*, 1996−2000.
24. Glickman, J. F., Pavlovich, J. G., and Reich, N. O. (1997) Peptide mapping of the murine DNA methyltransferase reveals a major phosphorylation site and the start of translation, *J. Biol. Chem. 272*, 17851−17857.
25. Leonhardt, H., Page, A. W., Weier, H. U., and Bestor, T. H. (1992) A targeting sequence directs DNA methyltransferase to sites of DNA replication in mammalian nuclei, *Cell 71*, 865−873.
26. Pedrali-Noy, G., and Weissbach, A. (1986) Mammalian DNA methyltransferases prefer poly(dI-dC) as substrate, *J. Biol. Chem. 261*, 7600−7602.
27. Bolden, A., Ward, C., Siedlecki, J. A., and Weissbach, A. (1984) DNA methylation. Inhibition of de novo and maintenance methylation in vitro by RNA and synthetic polynucleotides, *J. Biol. Chem. 259*, 12437−12443.
28. Glickman, J. F., Flynn, J., and Reich, N. O. (1997) Purification and characterization of recombinant baculovirus-expressed mouse DNA methyltransferase, *Biochem. Biophys. Res. Commun. 230*, 280−284.
29. Kawasaki, H., and Taira, K. (2004) Induction of DNA methylation and gene silencing by short interfering RNAs in human cells, *Nature 431*, 211−217.
30. Morris, K. V., Chan, S. W., Jacobsen, S. E., and Looney, D. J. (2004) Small interfering RNA-induced transcriptional gene silencing in human cells, *Science 305*, 1289−12892.
31. Jenuwein, T. (2002) Molecular biology. An RNA-guided pathway for the epigenome, *Science 297*, 2215−2218.
32. Carty, S. M., and Greenleaf, A. L. (2002) Hyperphosphorylated C-terminal repeat domain-associating proteins in the nuclear proteome link transcription to DNA/chromatin modification and RNA processing, *Mol. Cell Proteomics 1*, 598−610.
33. Jeffery, L., and Nakielny, S. (2004) Components of the DNA methylation system of chromatin control are RNA-binding proteins, *J. Biol. Chem. 279*, 49479−49487.
34. Muromoto, R., Sugiyama, K., Takachi, A., Imoto, S., Sato, N., Yamamoto, T., Oritani, K., Shimoda, K., and Matsuda, T. (2004) Physical and functional interactions between Daxx and DNA methyltransferase 1-associated protein, DMAP1, *J. Immunol. 172*, 2985−2993.
35. Liu, Z., and Fisher, R. A. (2004) RGS6 interacts with DMAP1 and DNMT1 and inhibits DMAP1 transcriptional repressor activity, *J. Biol. Chem. 279*, 14120−14128.
36. Kimura, H., and Shiota, K. (2003) Methyl-CpG-binding protein, MeCP2, is a target molecule for maintenance DNA methyltransferase, Dnmt1, *J. Biol. Chem. 278*, 4806−4812.
37. Fuks, F., Hurd, P. J., Deplus, R., and Kouzarides, T. (2003) The DNA methyltransferases associate with HP1 and the SUV39H1 histone methyltransferase, *Nucleic Acids Res. 31*, 2305−2312.
38. Fuks, F., Burgers, W. A., Brehm, A., Hughes-Davies, L., and Kouzarides, T. (2000) DNA methyltransferase Dnmt1 associates with histone deacetylase activity, *Nat. Genet. 24*, 88−91.
39. Fuks, F., Hurd, P. J., Wolf, D., Nan, X., Bird, A. P., and Kouzarides, T. (2003) The methyl-CpG-binding protein MeCP2 links DNA methylation to histone methylation, *J. Biol. Chem. 278*, 4035−4040.
40. Vilkaitis, G., Suetake, I., Klimasauskas, S., and Tajima, S. (2005) Processive Methylation of Hemimethylated CpG Sites by Mouse Dnmt1 DNA Methyltransferase, *J. Biol. Chem. 280*, 64−72.
41. Xu, G., Flynn, J., Glickman, J. F., and Reich, N. O. (1995) Purification and stabilization of mouse DNA methyltransferase, *Biochem. Biophys. Res. Commun. 207*, 544−551.
42. Svedruzic, Z. M., and Reich, N. O. (2004) The Mechanism of Target Base Attack in DNA Cytosine Carbon 5 Methylation, *Biochemistry. 43*, 11460−11473.
43. Wu, J. C., and Santi, D. V. (1987) Kinetic and catalytic mechanism of HhaI methyltransferase, *J. Biol. Chem. 262*, 4778−4786.
44. Pradhan, S., Bacolla, A., Wells, R. D., and Roberts, R. J. (1999) Recombinant human DNA (cytosine-5) methyltransferase. I. Expression, purification, and comparison of de novo and maintenance methylation, *J. Biol. Chem. 274*, 33002−33010.
45. Reale, A., Matteis, G. D., Galleazzi, G., Zampieri, M., and Caiafa, P. (2005) Modulation of DNMT1 activity by ADP-ribose polymers, *Oncogene 24*, 13−19.
46. Rountree, M. R., Bachman, K. E., and Baylin, S. B. (2000) DNMT1 binds HDAC2 and a new co-repressor, DMAP1, to form a complex at replication foci, *Nat. Genet. 25*, 269−277.

47. Easwaran, H. P., Schermelleh, L., Leonhardt, H., and Cardoso, M. C. (2004) Replication-independent chromatin loading of Dnmt1 during G2 and M phases, *EMBO Rep. 5*, 1181−1186.
48. Hermann, A., Goyal, R., and Jeltsch, A. (2004) The Dnmt1 DNA-(cytosine-C5)-methyltransferase methylates DNA processively with high preference for hemimethylated target sites, *J. Biol. Chem. 279*, 48350−48359.
49. Porter, D. J., Short, S. A., Hanlon, M. H., Preugschat, F., Wilson, J. E., Willard, D. H., Jr., and Consler, T. G. (1998) Product release is the major contributor to kcat for the hepatitis C virus helicase-catalyzed strand separation of short duplex DNA, *J. Biol. Chem. 273*, 18906−18914.
50. Ali, J. A., and Lohman, T. M. (1997) Kinetic measurement of the step size of DNA unwinding by *Escherichia coli* UvrD helicase, *Science 275*, 377−380.
51. Steinfeld, J. I., Francisco, J. S., and Hase, W. L. (1998) *Chemical Kinetics and Dynamics*, 2nd ed., Prentice Hall, New York.

BI050988F